Functional Ecology

Functional Ecology 2012, **26**, 1054–1065 doi: 10.1111/j.1365-2435.2012.02022.x

A species-level model for metabolic scaling in trees I. Exploring boundaries to scaling space within and across species

John S. Sperry*[,1], Duncan D. Smith[1], Van M. Savage[2,3], Brian J. Enquist[4], Katherine A. McCulloh[5], Peter B. Reich[6,7], Lisa P. Bentley[4] and Erica I. von Allmen[1]

[1]*Department of Biology, University of Utah, Salt Lake City, Utah, 84112 USA;* [2]*Department of Biomathematics, David Geffen School of Medicine, University of California, Los Angeles, California, 90095 USA;* [3]*Department of Ecology and Evolutionary Biology, University of California, Los Angeles, California, 90095 USA;* [4]*Department of Ecology and Evolutionary Biology, University of Arizona, Tucson, Arizona, 85721 USA;* [5]*Department of Forest Ecosystems and Society, Oregon State University, Corvallis, Oregon, 97331 USA;* [6]*Department of Forest Resources, University of Minnesota, St. Paul, Minnesota, 55108 USA; and* [7]*Hawkesbury Institute for the Environment, University of Western Sydney, Penrith, New South Wales, 2751 Australia*

Summary

1. Metabolic scaling theory predicts how tree water flow rate (Q) scales with tree mass (M) and assumes identical scaling for biomass growth rate (G) with M. Analytic models have derived general scaling expectations from proposed optima in the rate of axial xylem conduit taper (taper function) and the allocation of wood space to water conduction (packing function). Recent predictions suggest G and Q scale with M to the $\approx 0{\cdot}7$ power with $0{\cdot}75$ as an upper bound.

2. We complement this *a priori* optimization approach with a numerical model that incorporates species-specific taper and packing functions, plus additional empirical inputs essential for predicting Q (effects of gravity, tree size, heartwood, bark, and hydraulic resistance of leaf, root and interconduit pits). Traits are analysed individually, and in ensemble across tree types, to define a 2D 'scaling space' of absolute Q vs. its scaling exponent with tree size.

3. All traits influenced Q and many affected its scaling with M. Constraints driving the optimization of taper or packing functions, or any other trait, can be relaxed via compensatory changes in other traits.

4. The scaling space of temperate trees overlapped despite diverse anatomy and winter-adaptive strategies. More conducting space in conifer wood compensated for narrow tracheids; extensive sapwood in diffuse-porous trees compensated for narrow vessels; and limited sapwood in ring-porous trees negated the effect of large vessels. Tropical trees, however, achieved the greatest Q and steepest size-scaling by pairing large vessels with extensive sapwood, a combination compatible with minimal water stress and no freezing-stress.

5. Intraspecific scaling across all types averaged $Q \propto M^{0{\cdot}63}$ (maximum $= Q \propto M^{0{\cdot}71}$) for size-invariant root–shoot ratio. Scaling reached $Q \propto M^{0{\cdot}75}$ only if conductance increased faster in roots than in shoots with size. Interspecific scaling could reach $Q \propto M^{0{\cdot}75}$, but this may require the evolution of size-biased allometries rather than arising directly from biophysical constraints.

6. Our species-level model is more realistic than its analytical predecessors and provides a tool for interpreting the adaptive significance of functional trait diversification in relation to whole-tree water use and consequent metabolic scaling.

Key-words: ecological wood anatomy, functional tree types, hydraulic architecture, Metabolic scaling theory, plant allometry, tree water transport, vascular network theory, West Brown and Enquist

*Correspondence author. E-mail: j.sperry@utah.edu

Introduction

How does tree water use scale with tree size, and how does it differ across species? Given the essential role of water, this question is fundamental to understanding the metabolic scaling of individual trees, species, forest communities and ecosystems. Predicting the answer from vascular anatomy is the subject of this study. Modelling water use from vascular properties has a long history dating at least to da Vinci's rule of area-preserving branching (Richter 1970), continuing with the Ohm's law analogy of van den Honert (1948; Richter 1973) and culminating in the concept of 'hydraulic architecture' (Zimmermann 1978) represented in contemporary models (e.g. Tyree 1988; Sperry *et al*. 2002; Macinnes-Ng *et al*. 2011). At the heart of these complex models is a simple relationship for whole-tree sap flow at steady state (Q):

$$Q = K(\Delta P - \rho g H) \qquad \text{eqn 1}$$

where K is tree hydraulic conductance, ΔP is soil to canopy pressure drop, and $\rho g H$ is the pressure required to offset the force of gravity on the water column (ρ = density of water; g, acceleration of gravity; H, tree height). Canopy xylem pressure regulation (via stomatal control of Q) constrains the ($\Delta P - \rho g H$) term, and most of the uncertainty in hydraulic modelling lies in representing K which depends mostly on the complex anatomy of the flow path from soil to leaf.

Until the revolutionary approach of West, Brown and Enquist ('WBE'; West, Brown & Enquist 1997; Enquist, West & Brown 2000; West, Brown & Enquist 1999), most hydraulic modelling was based on specifying what K *is* from empirical inputs. In contrast, the WBE model derives what the allometric scaling of K *should be* by assuming a universal set of optimization criteria and an intentionally minimalist representation of plant vasculature. The WBE goal is to predict universal expectations for how K, and hence Q, and all dependent metabolic processes, should scale with plant size. The focus is on predicting the power function scaling exponent (b):

$$Y \propto M^b \qquad \text{eqn 2}$$

where Y is the variable of interest (K, Q, rates of metabolism or growth) and M is plant mass.

The result is a metabolic scaling theory that emphasizes the unifying consequences of selection for optimal vascular transport under overarching constraints. Savage *et al*. (2010) have recently extended the theory with important improvements in how it represents vascular architecture.

In this study, we present a model that strikes a middle ground between the structure-to-function optimization approach of Savage *et al*. (and its WBE predecessors) and the descriptive – empirical approach of more complex numerical models. We add a minimal set of hydraulic inputs to the Savage *et al*. analytical model with the goal of predicting the actual value of K and Q rather than proportional proxies that are sufficient for predicting scaling exponents. Our species-level model turns the proportionality in eqn 2 ($Y \propto M^b$) into an equality ($Y = k_0 M^b$) by specifying scaling multipliers (k_0). The additional complexity requires a numerical approach, but is justified because selection for optimal vascular function should concern traits underlying the multiplier as well as the exponent. Furthermore, variation in scaling multipliers across species could influence interspecific exponents (b) independently of the intraspecific value of b. We relax any *a priori* optimization criteria and allow key hydraulic inputs to be empirical, so that we can predict the 'scaling space' defined by variation in k_0 and b across species.

Figure 1 provides a roadmap of the Savage *et al*. (2010) model. The branching architecture component (Fig. 1, left) specifies that the tree has symmetric, self-similar branching architecture that preserves the cross-sectional area of branches across each branching junction (da Vinci's rule; Horn 2000). Hence, the tree can be represented by a column (Fig. 1, center). The mass allometry module predicts the best-fit power-law scaling between trunk diameter (D_{B0}; 0 denotes trunk branch rank; symbols in Table 1) and tree mass (M):

$$D_{B0} = k_1 M^c \qquad \text{eqn 3}$$

where k_1 is the scaling multiplier and c the scaling exponent. The value of the exponent c is derived from well-tested theory that H must scale with $D_{B0}^{2/3}$ for trees to maintain a constant safety margin from buckling under their own weight ('elastic similarity', McMahon 1973). An elastically similar column has a mass exponent of $c = 3/8$ in eqn 3 (West, Brown & Enquist 1997, 1999; Enquist, West & Brown 2000; Savage *et al*. 2010).

The water use allometry module predicts how the steady-state rate of midday xylem transport (Q) scales with trunk diameter:

$$Q = k_2 D_{B0}^q \qquad \text{eqn 4}$$

with multiplier k_2 and water use exponent, q. To obtain Q, the Hagen–Poiseuille equation (Zimmermann 1983) is used to calculate tree hydraulic conductance (K) from the number and dimensions of the xylem conduits in the tree sapwood, given by the xylem architecture module (Fig. 1, right). The prediction of K yields Q by eqn 1, and the scaling of Q with tree size yields the water use allometry of eqn 4. Previous derivations of the water use exponent q in eqn 4 have assumed that selection for transport efficiency has driven it to its theoretical maximum of $q = 2$ (for the assumed xylem architecture; West, Brown & Enquist 1999; Enquist, West & Brown 2000; Savage *et al*. 2010). At this point, the rate of whole-tree water transport depends solely on its trunk basal area and is not negatively influenced by tree height or transport distance ($Q \propto D_{B0}^2/H^0$).

The fifth metabolic isometry component of the Savage *et al*. model is a fundamental assumption of metabolic scaling theory: because photosynthetic CO_2 flux and

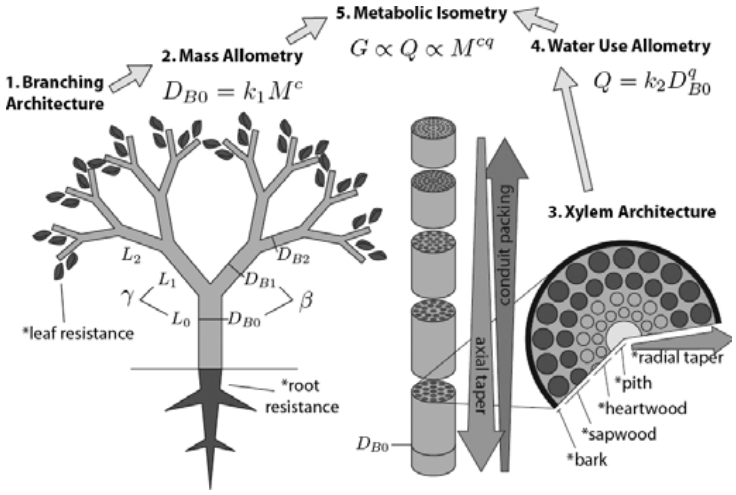

Fig. 1. Elements of metabolic scaling theory. Self-similar and symmetric branching architecture (left) that is area-preserving (central column) yields trunk diameter (D_{B0}) by mass (M^{c}) scaling. Xylem conduit architecture (shown in column cross-sections) yields water use (Q, flow rate) by D_{B0}^{q} scaling. Combining mass and water use yields Q by M^{cq} scaling. If growth rate (G) is isometric with Q (metabolic isometry), then the theory yields growth rate (G) by M^{cq} scaling. Asterisked components represent novel parameters that were not explicit in the Savage *et al.* (2010) model. See Table 1 for other symbols.

transpirational water flux are both limited by stomatal diffusion, gross photosynthesis and potential isometric surrogates such as total respiration and growth rate (G) should scale proportionally with Q (Enquist *et al.* 2007a). Combining metabolic isometry with the mass and water use allometries predicts metabolic scaling: $G \propto Q \propto M^{cq}$, where the metabolic scaling exponent is the product of the exponents for mass (c; eqn 3) and water use (q; eqn 4) scaling.

If $c = 3/8$ (from elastic similarity) and $q = 2$ (the theoretical Savage *et al.* maximum), the metabolic exponent $c{\cdot}q = 3/4$ (West, Brown & Enquist 1999; Enquist, West & Brown 2000). This prediction has provoked debate, partly over the validity of metabolic isometry and in partly regarding q (*e.g.* Meinzer *et al.* 2005; Reich *et al.* 2006; Enquist *et al.* 2007a; Sperry, Meinzer & McCulloh 2008). Metabolic isometry is addressed in the second paper of this series (von Allmen *et al.* 2012). Here, we focus on the derivation of q.

For $q \geq 2$ the negative effects of tree height and distance on Q must be eliminated. Height is negated if the drop in xylem pressure from soil to canopy (ΔP) compensates for gravity (ρgH), making the driving force ($\Delta P - \rho gH$; eqn 1) height-invariant. However, the ($\Delta P - \rho gH$) term often declines with height (Mencuccini 2003; Ryan Phillips & Bond 2006).

Transport distance can be negated by the 'bottleneck effect' where high flow resistance at the end of the xylem pipeline restricts the flow rate regardless of pipeline length. A bottleneck effect is consistent with the tapering of xylem conduits from trunk to terminal twig (West, Brown & Enquist 1999; Enquist, West & Brown 2000; Sperry, Meinzer & McCulloh 2008). This narrowing is captured in the Savage *et al.* model by a 'taper function': the conduit diameter inside the terminal twigs is assumed size-invariant and conduits widen proximally as the stems themselves widen across branch ranks (Fig. 1, downward 'axial taper' arrow).

The bottleneck effect is also influenced by how the number of conduits running in parallel changes across branch ranks. The Savage *et al.* model uses a 'packing function' (Sperry, Meinzer & McCulloh 2008) to govern the number of conduits that fit in a specified portion of wood space. Consequently, as conduits become narrower towards the twigs, their number per wood area increases (Fig. 1, upward 'conduit packing' arrow). To optimize space-filling, Savage *et al.* assume a universal packing function that allocates a constant fraction of wood space to transport vs. across all branch ranks. Savage *et al.* then solve for optimal conduit taper on the basis of an efficiency vs. safety trade-off (see also Enquist, West & Brown 2000). Taper is increased just enough to yield $q = 2$ (to maximize transport efficiency), but no more. Excessive taper would continue to widen conduits proximally, but to no effect other than to compromise safety from cavitation (larger conduits tend to be more vulnerable; Hacke *et al.* 2006).

Is the bottleneck effect enough to yield $q = 2$? Savage *et al.* recognize that not all species have identical taper and packing functions (McCulloh *et al.* 2010), suggesting that the space-filling and efficiency vs. safety trade-offs they invoke may have diverse context-dependent optima (Price, Enquist & Savage 2007). The intentional simplicity of the Savage *et al.* model also excluded additional variables that potentially influence the bottleneck effect such as the

Table 1. Major symbols and definitions

Symbols	Definitions
A_{Si}	Sapwood area, branch level i
A_S/A_T	Sapwood area/basal area for reference tree size with D_{B0} = 72 cm
C_F	Fraction of wood occupied by conduit lumens (conduit lumen fraction)
C	Xylem hydraulic conductance/Hagen–Poiseuille conductance (end-wall correction)
D_{B0}	Trunk diameter (branch rank 0)
D_{Bi}	Stem diameter for branch rank i
D_C	Xylem conduit diameter
$D_C\ max$	Maximum allowable conduit diameter
$D_C\ twig$	Conduit diameter in the distal-most branch rank (twigs)
D_P	Pith diameter
F	Number of conduits per wood area
g	acceleration of gravity
G	biomass growth rate of shoot
H/H_B	tree height/Euler buckling height
K	tree hydraulic conductance
K_L/K_T	Leaf hydraulic conductance/supporting twig conductance
K/K_S	Tree conductance/shoot conductance
k_0, b	Generalized scaling multiplier and exponent (e.g. $Y = k_0\ M^b$)
k_1, c	Mass scaling multiplier and exponent ($D_{B0} = k_1\ M^c$)
k_2, q	Water use scaling multiplier and exponent ($Q = k_2\ D_{B0}{}^q$)
k_3, p	Taper function multiplier and exponent ($D_C = k_3\ D_{Bi}{}^p$)
k_4, d	Packing function multiplier and exponent($F = k_4\ D_C{}^d$)
k_5, a	Bark thickness function multiplier and exponent ($T_{Bi} = k_5\ D_{Bi}{}^a$)
k_6, s	Sapwood area function multiplier and exponent ($A_{Si} = k_6\ D_{Bi}{}^s$)
L_i	Branch segment length, level i
M	Shoot (above-ground) mass
N_C	Conduit number
n	Daughter/mother branch number ratio
Q	Steady-state tree water transport rate at mid-day
Q_{ref}	Q for 'reference' tree size of trunk diameter D_{B0} = 72 cm
T_{Bi}	Bark thickness, branch level i
V	Shoot (above-ground) volume
β	Daughter/mother branch diameter ratio
ΔP	Total soil to canopy water potential difference
γ	Daughter/mother branch length ratio
η	Viscosity of water
ρ	Density of water

terminal resistance of leaves and the presence of nonconducting heartwood and bark.

The Savage *et al.* model also considers a basic issue in the derivation of q: the water use allometry only becomes a pure power function (e.g. eqn 4) at the limit of infinite tree size (Mencuccini *et al.* 2007). Thus, best-fit power functions across different size ranges yield different q (and c) exponents. For example, Savage *et al.* solve for the rate of conduit taper that is just sufficient to make $q = 2$ at the limit of infinite tree size, while the same taper yields only $q \approx 1{\cdot}86$ for finite-sized trees. This leads to their prediction of a metabolic scaling exponent of $c{\cdot}q \approx 0{\cdot}70$ (3/8·1·86) in trees of actual size, with $c{\cdot}q = 0{\cdot}75$ as an upper bound (Savage *et al.* 2010).

Our species model attempts to clarify some of the uncertainty in metabolic scaling theory by revisiting the derivation of the water use allometry component (eqns 1 & 4). New inputs of xylem architecture and function (asterisks in Fig. 1, see Model Description) are added to the Savage *et al.* framework to improve q estimation and to enable the prediction of the k_2 multiplier so that actual flow rates, Q, can be estimated. We focus on how specific hydraulic traits can effect the scaling of water use. For simplicity, we do not alter the branching architecture of the Savage *et al.* model (2010). We apply the new model to four objectives. (i) Using the simpler Savage *et al.* parameterization, we quantify the effects of finite tree size and gravity (i.e. the $[\Delta P - \rho gH]$ term) on intraspecific scaling. (ii) We determine the influence of new inputs and variable taper and packing on the water use exponent (q) and multiplier (k_2). (iii) We translate how interspecific variation in wood traits translates into a map of 'scaling space' – defined by all possible combinations of multipliers (k_2) and the exponents (q) across species. The scaling space was simulated for four major functional tree types: conifers, ring-porous- and tropical and temperate diffuse-porous-angiosperms. (iv) Ecological drivers of scaling diversity are discussed, as are the implications for ¾ power metabolic scaling within vs. across species. The second paper tests the model against empirical measurements (von Allmen *et al.* 2012).

Model description

The model has 17 inputs, with default values listed in Table 2. The model was written as a macro in Microsoft Excel using Visual Basic for Applications and is available from the senior author.

BRANCHING ARCHITECTURE AND MASS ALLOMETRY

Trees are represented as a symmetrically self-similar structure shown in Fig. 1 (left). Branches at level i (counting from $i = 0$ at the trunk) are identical in length and diameter. Area-preservation (da Vinci's rule; Horn 2000) sets the ratio of daughter/mother branch diameter (β) at $\beta = n^{-1/2}$, where n is the daughter/mother branch number ratio (Table 1 defines all symbols). Elastic similarity, which requires $H \propto D_{B0}{}^{2/3}$ (McMahon 1973), sets the daughter/mother branch length ratio (γ) at $\gamma = n^{-1/3}$. Modelled trees converge on elastic similarity with size as observed (Niklas & Spatz 2004).

Dimensions of the terminal branch rank (twigs) are assumed constant regardless of tree size. Twig diameter set to 2 mm. Twig length was selected to yield convergence in large trees on the desired safety factor from buckling (H_B/H). The height at elastic buckling (H_B) was calculated according to Niklas (1994). Simulated 'species' had identical branch architecture inputs (default β, γ, n, H_B/H, twig diameter, twig length; Table 2). The mass scaling exponent (c) was obtained from the slope of log-log plots of D_{B0} vs. tree volume ($V = \pi\ D_{B0}{}^2\ H/4$) across networks of different

Table 2. Model inputs and outputs in order of appearance in text. Power functions were used for their simplicity and good fit to empirical trends

Input	Default
n, branch number ratio	2
γ, branch length ratio	0·794 (elastic similarity for $n = 2$ symmetric branching)
β, branch diameter ratio	0·707 (area-preserving $n = 2$ symmetric branching)
H_B/H, mature tree safety factor	4
Terminal twig diameter	2 mm
Terminal twig length	8·1 cm
$D_C = k_3 D_{Bi}^p$; taper function	k_3 = 7·9 μm mm^{-p}, p = 1/3; D_C in μm, D_{Bi} in mm
D_C *max*	240 μm
D_C *twig*	10 μm
$F = k_4 D_C^d$; packing function	k_4 = 100 000 μm^{-d} mm^{-2}; d = -2; F in mm^{-2}, D_C in μm
D_P, pith diameter	1 mm
$T_{Bi} = k_5 D_{Bi}^a$ bark function	k_5 = 0·0225 mm$^{(1-a)}$; a = 1·05; T_{Bi} and D_{Bi} in mm
$A_{Si} = k_6 D_{Bi}^s$; sapwood function	k_6 = 0·905 mm$^{(2-s)}$; s = 1·93; A_{Si} in mm^2, D_{Bi} in mm
C, end-wall correction factor	0·44 (angiosperms); 0·36 (conifers)
K_L/K_T, leaf/twig conductance	0·30
K/K_S, tree/shoot conductance	0·50
ΔP, total pressure drop	1 MPa
Outputs	
H, D_{B0} and V, yielding estimates of c: $D_{B0} \propto M^c$	
K and D_{B0}	
Q and D_{B0}, yielding estimates of q: $Q = k_2 D^q$	
Estimates of $G \propto Q \propto M^{cq}$	

size. We did not specify the multiplier k_1 for intraspecific scaling. However, for simulations of interspecific scaling, k_1 across species was specified by assuming branch tissue density equalled wood density (Appendix S1-III in Supporting Information).

XYLEM ARCHITECTURE AND WATER USE ALLOMETRY ($Q = K_2 D_{B0}^{\ Q}$)

The 'taper function' describes how xylem conduit diameter (D_C, μm) increases with stem diameter (D_{Bi} mm):

$$D_C = k_3 D_{Bi}^p \qquad \text{eqn 5}$$

where p is the 'taper exponent' and k_3 (μm mm^{-p}) the multiplier. The default $p = 1/3$ is the smallest p yielding $q = 2$ at the limit of infinite tree size in the Savage *et al.* model (Savage *et al.* 2010). The choice of the minimum D_C in the terminal twigs dictated k_3 (default D_C *twig* = 10 μm, Table 2). When the model was run with axial taper alone (as in the Savage *et al.* model), D_C narrows as D_{Bi} narrows, but is constant from pith to cambium at a given branch level (Fig. 1, downward 'axial taper' arrow). When radial taper is added, D_C increases from pith to cambium, starting from $D_C = D_C$ *twig* and increasing with the taper function as branch diameter is incremented (in 100 μm steps) to D_{Bi} (Fig. 1, enlarged cross-section). To avoid unrealistically large D_C, a maximum (Table 2, D_C *max*) was set. Default D_C *max* was set to 240 μm because this was the greatest D_C in our functional type survey (Table 3; Appendix S1-II in Supporting Information).

The number of xylem conduits per xylem area (F, mm^{-2}) was calculated from conduit diameter (D_C, μm) using the 'packing function' (Sperry, Meinzer & McCulloh 2008):

$$F = k_4 D_C^d \qquad \text{eqn 6}$$

where d is the packing exponent (a negative number) and k_4 (mm^{-2} μm^{-d}) the multiplier. The choice of k_4 dictated the fraction of the total wood area occupied by xylem conduits ($C_F < 1$). For square packing (one conduit per square of space), maximum $F = 10^6\ D_C^{\ -2}$ and $C_F = [\ k_4/\ 10^6\ ]\ D_C^{\ (d+2)}$. Savage *et al.* assumed an optimal $d = -2$ (our default), such that C_F is constant from twig to trunk (or pith to cambium). The default k_4 (Table 2) was chosen to yield $C_F = 0{\cdot}1$, a typical hardwood value (McCulloh *et al.* 2010). If d was less negative than -2, then C_F increased from twig to trunk and vice-versa for d more negative than -2.

Xylem cross-sectional area was obtained by subtracting the bark and pith area from total branch area. Pith diameter (D_P, mm) was invariant within a tree, with a default of 1 mm. The bark thickness at level i (T_{Bi}, mm) was calculated from branch diameter (D_{Bi}, mm) as:

$$T_{Bi} = k_5 D_{Bi}^a \qquad \text{eqn 7}$$

where a is the bark exponent and k_5 (mm$^{(1-a)}$) the multiplier. For simplicity, we restricted the analysis of bark thickness to the two bark functions used to test the model in the companion paper (von Allmen *et al.* 2012). These were from a relatively thin-barked maple (*Acer grandidentatum*) and a thicker-barked oak (*Quercus gambelii*). Maple served as the default (Table 2).

Total xylem area was divided into nonconducting heartwood and conducting sapwood. The sapwood area (A_{Si}, mm^2) at level i from branch diameter (D_{Bi}, mm) is given by:

$$A_{Si} = k_6 D_{Bi}^s \qquad \text{eqn 8}$$

where s is the sapwood exponent and k_6 (mm$^{(2-s)}$) the multiplier. The exponent s has a maximum of $s = 2$ to avoid sapwood area from exceeding xylem area and a minimum of $s = 1$ for thin sapwood of approximately constant depth. Values of k_6 and s were obtained from the companion paper on oak and maple (von Allmen *et al.* 2012) and the sapflux literature. Sapwood functions were adjusted to have heartwood first appear at $D_{Bi} = 2{\cdot}2$ cm and expand to reduce sapwood to varying percentages of total basal area at $D_{B0} = 72$ cm. The default percentage was 74%.

Table 3. Model inputs used to define the hydraulic scaling of four tree types (Fig. 4). Ranges adapted from the literature (Appendix S1-II in Supporting Information). Additional inputs were set to defaults listed in Table 2. The A_S/A_T trunk is the fraction of sapwood area per basal area in a tree of D_{B0} = 72 cm that results from the inputted sapwood function. Note that the range of leaf-to-twig conductance ratio (K_L/K_T) was assumed to be the same for all categories, as were the sapwood parameters in all but the ring-porous category.

	Ring-porous temperate	Diffuse-porous temperate	Diffuse-porous tropical	Conifers
D_C *twig*, μm	21 (16·8–25·2)	12 (9·6–14·4)	21 (16·8–25·2)	7 (5·6–8·4)
D_C *max*, μm	145–240	33–79	158–240	28–45
Taper p	0·30–0·59	0·14–0·41	0·31–0·61	0·20–0·44
Packing d	−1·34 to −2·29	−1·65 to −3·27	−2·38 to −2·0	−1·69 to −1·8
C_F	0·09–0·37	0·07–0·20	0·06–0·12	0·37–0·42
K_L/K_T	0·20–0·40	0·20–0·40	0·20–0·40	0·20–0·40
Sapwood s	1·05–1·36	1·55–1·91	1·55–1·91	1·55–1·91
A_S/A_T trunk	0·003–0·017	0·34–0·74	0·34–0·74	0·34–0·74

This corresponded to a default sapwood depth from the cambium of 18·9 cm. Power functions for eqns 5-8 were chosen because of their convenience and good fit to empirical trends. The hydraulic conductance of a branch (K_{Bi}) was calculated from branch length (L_i, μm), and the number (N_C) and diameter (D_C, μm) of xylem conduits, using the Hagen–Poiseuille equation. Conduit number was obtained from the packing function and the sapwood area. When the model was run with radial D_C taper, we integrated the Hagen–Poiseuille equation from the inner sapwood boundary ($x = 0$) to the cambium ($x = rc$) to yield the K_{Bi}:

$$K_{Bi} = C \int_{x=0}^{x=rc} N_C(x)\pi[D_C(x)]^4/(128\eta Li)dx \qquad \text{eqn 9}$$

where N_C (x) and D_C (x) are functions of the radial distance x across the sapwood according to the packing and taper functions. The integral was solved numerically by 100 μm increments in x (smaller increments were unnecessary). The viscosity, η, was set at 0·001 Pa s for 20°C. The dimensionless constant C is an empirical correction factor ($0 < C < 1$) that accounts for interconduit flow resistance. The literature yielded default correction factors of C = 0·44 (angiosperms; Hacke *et al.* 2006) and C = 0·36 (conifers; Pittermann *et al.* 2005). Branch K_{Bi} was multiplied by the number of branches in level i to yield the parallel conductance of rank i. Rank conductances in series gave the hydraulic conductance of the stem network.

Leaf and root system conductances were extrapolated from the branch network conductance. Leaf conductance was given by ratio of leaf conductance per twig conductance (K_L/K_T), which was assumed to be size-invariant. This ratio is not often measured, but values from *Acer grandidentatum* and *Quercus gambelii* cited in the companion paper (von Allmen *et al.* 2012) provided a range. A similar approach was used to incorporate root system conductance. The shoot conductance (K_S, all branches plus leaves) was multiplied by the ratio of tree–shoot conductance (K/K_S) to obtain the whole-tree (root plus shoot) conductance. The default K/K_S ratio was 0·5 in keeping with observations from a variety of woody plants (Sperry *et al.* 2002). The default was size-invariance of K/K_S, but we also allowed it to increase with size (Martinez-Vilalta *et al.* 2007).

Steady-state tree water transport rate (Q, kg hr^{-1}) at midday was calculated from tree conductance using eqn 1. Default ΔP = 1 MPa (Mencuccini 2002), making it size-invariant as seen for *Acer grandidentatum* and *Quercus gambelii* (von Allmen *et al.* 2012). Thus, the (ΔP-ρgH) driving force decreased with tree size. In an alternative 'gravity compensation' scenario, the (ΔP-ρgH) term was size-invariant. These two options cover the range of gravity responses of trees (see Discussion). The Savage *et al.* model and earlier models (West, Brown & Enquist 1997, 1999; Enquist *et al.* 2000) assume isometry between Q and K, thus implicitly adopting gravity compensation. Linear regressions of log-transformed Q vs. D_{B0} data yielded the water use allometry equation: $Q = k_2 D_{B0}{}^q$.

Model results

SIZE-DEPENDENT WATER USE ALLOMETRY

We investigated size effects using the model parameterized as in Savage *et al.*: no pith, sapwood or bark, no leaves or roots and no radial taper (Table 2 shows remaining default inputs). The only difference from Savage *et al.* was that we allowed for gravitational effects.

Size effects had two causes: juvenile growth that was not elastically similar (Appendix S1-I, Fig. S-1 in Supporting Information) and gravitational reduction in (ΔP-ρgH) in tall trees. In combination, these created a nonlinear (in log-log space) water use allometry (Q) with trunk diameter (D_{B0}; Fig. 2). In small trees, a power-law fit gave an approximate scaling exponent of $Q \propto D_{B0}{}^{q = 1{\cdot}12}$ (Fig. 2, grey). The exponent increased to a maximum as elastic similarity was approached in medium-sized trees: $Q \propto D_{B0}{}^{q = 1{\cdot}72}$ (Fig. 2, dark grey). In large trees, the exponent decreased as gravity (ρgH) subtracted an increasing portion of the pressure difference between soil and canopy (ΔP = 1 MPa, Table 2). Thus, Q scaling

became flatter in tall trees: $Q \propto D_{B0}{}^{q = 0{\cdot}91}$ (Fig. 2, black).

In the gravity compensation scenario, ΔP increased with H such that the (ΔP-ρgH) term was size-invariant and Q scaling did not flatten. Instead it reached $Q \propto D_{B0}{}^{q = 1{\cdot}86}$ in large sized trees (Fig. 2, dash-dotted no g line) as estimated for the Savage *et al.* model at their optimal taper ($p = 1/3$). Increasing tree size towards infinity gave the $q = 2$ asymptote (Savage *et al.* 2010).

INFLUENCE OF INDIVIDUAL TRAITS ON WATER USE SCALING

New variables added to the Savage *et al.* framework altered water use scaling. We report effects on the exponent, q, and the multiplier, k_2, for medium-sized trees ($2 < D_{B0} \leq 72$ cm) where Q by D_{B0} scaling was nearly linear in log-log space (Fig. 2). Rather than cite k_2 values, we substitute a more intuitive proxy: the rate of water transport at a reference tree size (Q_{ref} for $D_{B0} = 72$ cm).

Although the effects were quantitatively complex (Fig. 3), the take-home message is simple. All variables influenced $Q_{\rm ref}$ because they either increased tree hydraulic conductance (*e.g.* more, wider functioning conduits, higher leaf or root conductances) or reduced it (fewer, narrower functioning conduits, lower leaf or root conductances). A subset also altered q because they influenced the bottleneck effect: either increasing the difference in distal-to-proximal balance of hydraulic conductance in the shoot (greater q) or decreasing it (lower q). One variable (size-dependent K/K_S) altered q independently of the bottleneck effect.

Figure 3(a) shows the cumulative effect of adding new variables. Incorporating pith and bark (defaults in Table 2) reduced Q_{ref} by reducing xylem cross-sectional area, with thicker bark having a greater effect (Fig. 3a);

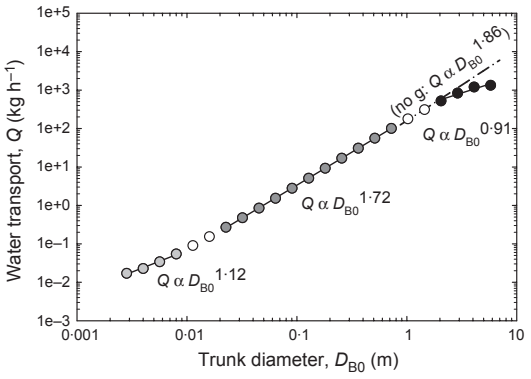

Fig. 2. Size-dependent variation in the q exponent ($Q \propto D_{B0}{}^{q}$) for tree water flow rate (Q) and trunk diameter (D_{B0}) in modelled trees. Small trees exhibit flat scaling because of the nonelastically similar growth of juveniles. Medium trees are steepest because they are elastically similar and have small gravity effects. The tallest trees flatten again because of larger gravity effects, unless there is gravity compensation (dash-dotted no g line).

q was not materially changed. Adding radial taper to the thin-barked default model decreased Q_{ref} further (Fig. 3a, radial taper) because of the narrowing of vessel diameter towards the pith; again, q changed little. Adding heartwood reduced both Q_{ref} and q (Fig. 3a, sapwood%). Reducing basal sapwood area from 74 to 30% (reducing sapwood thickness from 18·9 to 6·1 cm) caused q to drop from 1·72 to below 1·64 and Q_{ref} to drop by 24% (Fig. 3a). Heartwood decreased Q_{ref} by reducing the cross-sectional area for water conduction. Most of this reduction was in the larger branches and trunk, which decreased the bottleneck effect of the distal branches and lowered q.

The 74% basal sapwood function was adopted as the default (Table 2) for assessing the further effect of adding leaves in Fig. 3(b). As the K_L/K_T ratio was decreased from 1 to 0·01, Q_{ref} dropped by over 80% relative to the default no-leaf model (Fig. 3b) because leaves reduced network conductance. The reduction was at the distal end, which increased the bottleneck effect, and q increased from 1·72 to 1·92. The measured K_L/K_T range was relatively narrow: from 0·27 in *Quercus gambelii* to 0·38 in *Acer grandidentatum* (von Allmen *et al.* 2012).

The intervessel resistance factor (C, eqn 9) caused a proportional change on Q_{ref}, but no change in q because it did not influence the bottleneck. The same was true for adding below-ground resistance (Table 2, $K/K_S = 0{\cdot}50$). However, if K/K_S was allowed to increase with D_{B0} as estimated for *Pinus sylvestris* ($K/K_S = 0{\cdot}75\ D_{B0}{}^{0{\cdot}36}$ from Martinez-Vilalta *et al.* 2007), q rose to 2·12. This was the only input that gave $q \geq 2$. It did so not by increasing the shoot bottleneck effect, but because root conductance increased faster than shoot conductance with size.

Varying taper and packing from the universal functions assumed by Savage *et al.* was simulated for a default $K_L/K_T = 0{\cdot}30$ (Table 2; grey symbol in Fig. 3c,d). Fig. 3(c) shows the effect of taper. The default taper was $D_C = 7{\cdot}9\ D_{Bi}{}^{p = 1/3}$, corresponding to D_C *twig* = 10 μm. D_C *twig* was held constant while varying the taper exponent, p, by adjusting the multiplier. Decreasing taper from $p = 1/3$ to $p = 0{\cdot}2$ resulted in narrower conduits proximally, which reduced network conductance (51% drop in Q_{ref}) and the bottleneck effect (decrease in q from 1·76 to 1·59). Increasing taper above p = 1/3 had the opposite effect: Q_{ref} increased by almost 5-fold and q rose to 1·93. At $p \geq 0{\cdot}6$, conduit diameter in the proximal trunk and branches had to be capped at $D_C\ max$ = 240 μm (Fig. 3c, asterisked points). Saturation in q and Q_{ref} occurred at $p > 9$ because vessels had reached the 240 μm cap at every branch rank except the twigs. The 240 μm cap, heartwood and gravity prevented q from saturating at $q = 2$.

Figure 3(d) shows the influence of the packing function, $F = k_4\ D_C{}^{d}$. The greater the value of coefficient k_4, the greater the fraction of wood area devoted to water conduction (C_F). Increasing C_F caused a proportional increase in $Q_{\rm ref}$ (C_F = 0·01 to 0·6) with no effect on q (Fig. 3d). When varying the packing exponent d, we covaried the multiplier

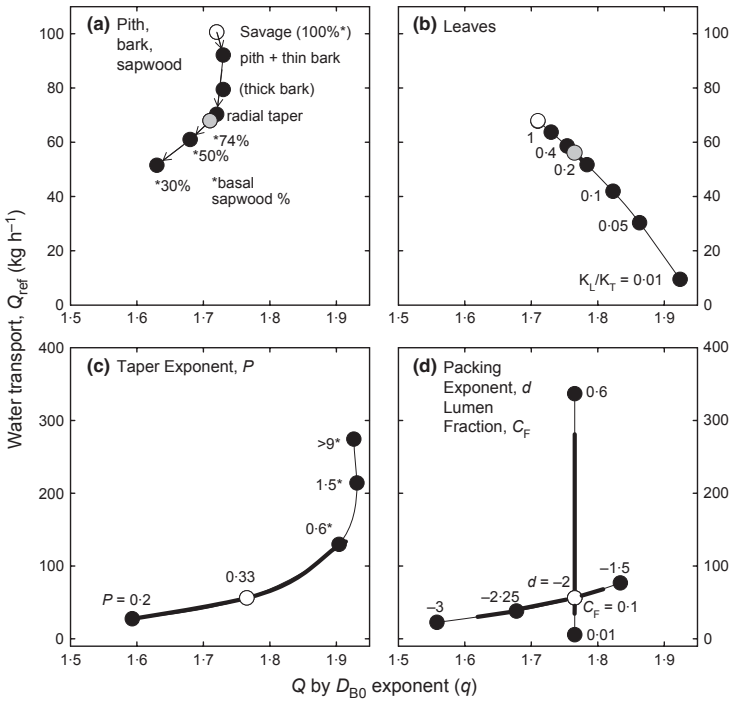

Fig. 3. Effect of individual hydraulic traits on tree flow rate (Q_{ref}, at trunk diameter D_{B0} = 72 cm), and the Q by $D_{B0}{}^{q}$ scaling exponent, q, for medium-sized trees. (a) Cumulative effects of adding pith and thin bark, radial taper and sapwood of decreasing percentage of basal area (at D_{B0} = 72 cm) to the Savage *et al.* model (open symbol). Thick bark shown separately. Grey 74% sapwood point is default for B. (b) Adding leaves of decreasing conductance (K_L) relative to twigs (K_L/K_T) decreased Q_{ref} and increased exponent q. Thick line is probable range of K_L/K_T, grey datum is default K_L/K_T (0·3) for C,D. (c) Increasing the conduit diameter taper exponent, p, makes wider conduits proximally (eqn 5) and increased Q_{ref} and q. Open symbol is default. Asterisked p exponents required proximal conduits to be capped at D_C *max* = 240 μm. Thick line is realistic range of exponent, p. (d) Varying the packing exponent, d, (eqn 6) had a large effect on the q exponent, but little effect on Q_{ref} compared to changing the fraction of conducting wood area (C_F). Thick lines indicate realistic ranges of d and C_F.

to keep C_F constant in the terminal twigs. Increasing d (less negative), resulted in more big trunk vessels and hence increased both the relative flow rate (Q_{ref}) and the Q by $D_{B0}{}^{q}$ scaling exponent. Decreasing the exponent had the opposite effect (Fig. 3d, d = −2·5 to −1·5). Effects of the exponent on Q_{ref} were small compared with the effect of conducting area fraction, C_F.

FUNCTIONAL TREE TYPES IN SCALING SPACE

While Fig. 3 isolates the consequences of particular traits, actual scaling integrates variation across all traits at once to create a 2D cloud of species-specific Q_{ref} by q combinations. We used the model to circumscribe this 'scaling space' for major tree categories: ring-porous temperate, diffuse-porous temperate, diffuse-porous tropical and conifers. For each category, we estimated the range for input variables for which multispecies data were available (Table 3; Appendix S1-II in Supporting Information); remaining inputs, including K/K_S, were defaults (Table 2). A version of the model (available from the second author) scanned input combinations that defined the extremes of Q_{ref} and q for medium-sized trees ($2 < D_{B0} \leq 72$ cm).

The four tree categories occupied distinct, but substantially overlapping, scaling space (Fig. 4). The most efficient transporters, with the greatest Q_{ref} and scaling exponent q, were the tropical diffuse-porous trees (Fig. 4, green DP tropical outline). Tropical trees combined largest trunk and twig vessels with extensive sapwood area. The only parameter compromising efficiency in tropical trees was a somewhat lower C_F (Table 3; fewer vessels per sapwood area).

Temperate ring-porous angiosperms achieved the next highest Q_{ref} (Fig. 4, black RP outline). Although their vessel diameter is similar to tropical trees, their limited sapwood area (Table 3) compromised transport and contributed to their broad q range. Their broad Q_{ref} range corresponded to a wide range in C_F (Table 3). Ring-porous trees overlapped considerably with their chief cohabitants, the temperate diffuse-porous angiosperms (Fig. 4, red DP temperate outline). Although temperate diffuse-porous trees have narrower vessel diameters than ring-porous

trees, this was compensated by their greater sapwood area (Table 3).

The most surprising result was the performance of the conifers (Fig. 4, blue conifer outline). Although conifer tracheids have by far the narrowest conduit diameter range, they compensate by having high C_F (Table 3), owing to the double role of tracheids in water transport and mechanical support. The high C_F of conifers placed them almost entirely within the transport capacity of temperate diffuse-porous angiosperms.

Assuming 'metabolic isometry', the hydraulic scaling in Fig 4 predicts growth rate scaling with tree mass ($G \propto M^{cq)}$. Assuming $c = 0{\cdot}369$ for medium-sized trees (Appendix S1-I in Supporting Information), the range for the $G \propto M^{cq}$ exponent was mapped onto the four tree types in Fig. 4 ($c{\cdot}q$ values on upper axis). The metabolic scaling exponents ranged from 0·26 to 0·71 and excluded three-fourth power scaling.

INTRASPECIFIC VS. INTERSPECIFIC SCALING

Each Q_{ref} by q coordinate in the scaling space of Fig. 4 corresponds to a unique water use allometry ($Q = k_2\ D_{B0}^{\ q}$; eqn 4) of a theoretical 'species'. Each species also has a potentially unique mass allometry ($D_{B0} = k_1\ M^{c}$) because of interspecific variation in wood density (Appendix S1-III in Supporting Information). These 'species' were sampled to simulate intraspecific vs. interspecific scaling of the metabolic $c{\cdot}q$ exponent. Theoretical species with $q < 1{\cdot}5$ were excluded because they are unlikely to exist (see Appendix S1-III in Supporting Information and Discussion).

When species were chosen at random and assumed to reach the same maximum size regardless of Q_{ref} and q, the intraspecific $c{\cdot}q$ averaged 0·63 ± 0·0011 (mean ± SE, $n = 1000$ trees) and the interspecific $c{\cdot}q$ averaged 0·66 ± 0·0018 (Fig. 5, 'random'). Both intraspecific and interspecific exponents fell short of $c{\cdot}q = 0{\cdot}75$.

In an alternative 'height-biased' sampling, we assumed that species from the upper right corner of scaling space in Fig. 4 (greater Q_{ref} and q) would have less of a hydraulic limitation on their maximum height and grow taller than species towards the lower left corner. Average intraspecific scaling was no different from the random scenario ($c{\cdot}q = 0{\cdot}63 \pm 0{\cdot}0020$), but the interspecific $c{\cdot}q$ could be significantly steeper depending on the sensitivity of species stature to their water use allometry and the size distribution of the interspecific sample. The particular case shown (see Appendix S1-III in Supporting Information for details) shows that interspecific $c{\cdot}q$ can match 3/4 power scaling ($c{\cdot}q = 0{\cdot}75 \pm 0{\cdot}0041$; Fig 5; 'height-biased').

Discussion

The model answers our opening question by providing species-specific predictions of the water use multiplier (k_2) and scaling exponent (q) in the water use allometry equation: $Q = k_2\ D_{B0}^{\ q}$. Greater k_2 indicates greater water transport, gas exchange and growth as predicted by metabolic scaling theory and shown empirically (e.g. Hubbard *et al.* 2001). A larger scaling exponent q means a greater rate of increase in these presumably competitive capacities with tree size (Hammond & Niklas 2012). In general, fertile and consistently moist habitats with low threat of cavitation

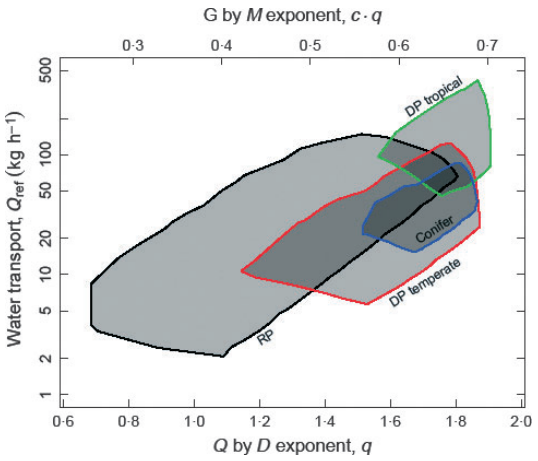

Fig. 4. Scaling space showing tree water transport rate (Q_{ref}, at trunk $D_{B0} = 72$ cm) and the scaling exponent q ($Q \propto D_{B0}^{\ q}$) for conifers (blue), temperate diffuse-porous (red), ring-porous (black, RP) and tropical trees (green). The corresponding growth rate by mass exponent ($c{\cdot}q$) is given on the upper axis. Parameter ranges defining these tree types are given in Table 3.

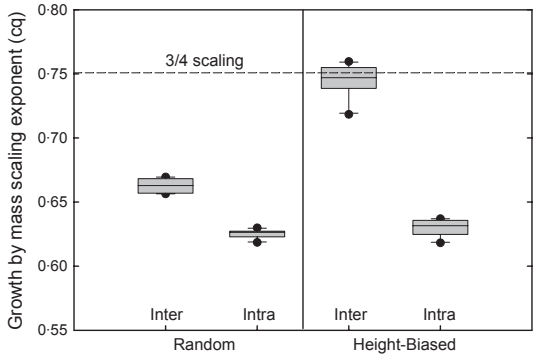

Fig. 5. Interspecific vs. intraspecific metabolic scaling exponents ($c{\cdot}q$) from n = 10 repetitions of the regression in Fig. S-2 (Appendix S1-III in Supporting Information). Symbols are outliers, whisker is 10th/90th percentile, box is 25th/75th percentile, line is median. Intraspecific scaling is not influenced by whether there was a random relationship between species scaling and stature, or a height-biased relationship where species with steeper and higher scaling (upper right of Fig. 4 scaling space) also reached greater size. The latter 'height-biased' scenario greatly steepened interspecific scaling and was the only interspecific sampling scheme that could yield exponents matching three-fourth power scaling (dashed line).

should favour conducting efficiency over safety. Species adapted to such habitats should cluster towards the upper right portions of Q_{ref} by q scaling space of Fig. 4. Conversely, arid and freezing habitats should push species to the lower left towards greater safety but lower transport capacity.

The considerable overlap in scaling space between the functional tree types exemplifies how trait variation presumably arises from ecological and evolutionary circumstances, and how divergence in scaling space is minimized by compensation between traits (Marks & Lechowicz 2006). Despite the overlap, tropical trees were distinguished by reaching the greatest maximum capacity by having large vessels with a long functional lifetime (= large sapwood areas). These features are consistent with selection favouring efficiency over safety in their relatively permissive habitat where the threat of cavitation by freezing or water stress is low (McCulloh *et al.* 2010).

The temperate diffuse- and ring-porous trees had lower peak transport capacities than the tropical trees. Accordingly, their habitat is not so permissive, certainly not in the case of freezing-induced cavitation. The adaptation to winter freezing takes different forms in ring- vs. diffuse-porous types (Sperry *et al.* 1994). Ring-porous trees had essentially the same range of vessel diameters and taper exponents as tropical trees, but the large vessels are sacrificed annually to cavitation by freezing. Hence, their drop in predicted transport capacity (lower Q_{ref}) and flatter scaling (lower q) relative to tropical trees results from giving up sapwood area.

Diffuse-porous temperate trees arguably adapted to freezing by having vessels narrow enough to limit the extent of cavitation (and many also reverse cavitation in spring; Hacke & Sauter 1996; Sperry *et al.* 1994). Their drop in transport capacity relative to tropical trees results from narrower vessels and less taper rather than less sapwood area. Both ring- and temperate diffuse-porous adaptations to freezing result in fairly similar estimated transport capacities: short-functioning and hence few, large vessels in ring-porous trees roughly equated to long-functioning and hence numerous, narrow vessels in diffuse-porous trees.

The conifers exhibit convergent scaling with temperate angiosperms despite very divergent wood structure. Their unicellular tracheids are limited in diameter for developmental and mechanical reasons compared with multicellular vessels (Pittermann *et al.* 2006). Hence tracheid taper functions are flatter (lower p range, Table 3). The greater impact of interconduit pits in conifers (lower C, Table 2) is because tracheids are much shorter than vessels and water encounters more interconduit walls as it flows through a given length of branch. But these disadvantages are largely compensated for by the efficiency of the torus-margo structure of their intertracheid pitting (Pittermann *et al.* 2005). The narrow tracheid diameters and low taper are made up for by maximally efficient packing functions (Sperry, Meinzer & McCulloh 2008). Conifer wood is a honeycomb of tracheids and consequently has a much greater conducting area (C_F up to 0·42, Table 3) than angiosperm xylem with its vessels dispersed in a fibre-parenchyma matrix ($C_F < 0{\cdot}37$). Conifer wood partially dodges the efficiency vs. safety trade-off by increasing efficiency with conduit number rather than conduit diameter.

Conifers also had packing exponents consistently less negative than $d = -2$ (Table 3; McCulloh *et al.* 2010), leading to a high water use exponent (q) despite their low taper exponent (p) range. Less negative d in conifers means there is a greater fraction of space devoted to water conduction in trunks vs. twigs. Anatomically, this is likely owing to a lower ratio of tracheid wall thickness: tracheid lumen diameter ('thickness-to-span' ratio) in trunks vs. twigs. The thickness-to-span ratio in turn scales with the strength of tracheids against implosion by internal negative sap pressures (Hacke *et al.* 2001). Thus, low thickness-to-span in trunk tracheids corresponds with less negative sap pressures proximally and vice-versa in the distal twigs.

If the model predictions are realistic, actual trees should fall within the boundaries shown in Fig. 4, but not necessarily fill them, because not all modelled trait combinations may have evolved. Indeed, data on intraspecific q, while limited, appear to primarily fall within the upper portion of the predicted range. Values of q much below ca. 1·5 have not been observed in trees (Enquist, West & Brown 2000; Mencuccini 2003; Meinzer *et al.* 2005; Sperry, Meinzer & McCulloh 2008), which is why lower values were excluded for assessing interspecific scaling. Flow rates for trees of ca. 72 cm in diameter (ca. 4 to 125 kg hr^{-1}) are also consistent with the predicted Q_{ref} range (Enquist, Brown & West 1998; Wullschleger, Meinzer & Vertessy 1998; Meinzer *et al.* 2005). A review of whole-tree water use in 67 species indicated no systematic differences in daily tree water use vs. trunk diameter between the four functional types we considered (Wullschleger, Meinzer & Vertessy 1998), which is consistent with their extensive overlap in Q_{ref} (Fig. 4). The predicted similarity of temperate tree types is supported by observed parity in whole-tree hydraulic conductance between temperate conifers and temperate angiosperms (Becker, Tyree & Tsuda 1999). Where differences have been seen between categories, they support model predictions. Tropical angiosperm trees in one extensive comparison moved more water per diameter than temperate conifers, consistent with our model results (Meinzer *et al.* 2005). A more direct test of the model in a diffuse- and a ring-porous species is the subject of the second paper in this series (von Allmen *et al.* 2012).

The functional type simulations indicate that there are multiple ways to 'skin the cat' when it comes to achieving a given water transport capacity and size-scaling. The Savage *et al.* derivation of an optimal taper ($p = 1/3$, eqn 5) effectively captures the consequences of conduit taper while holding other variables constant (Savage *et al.* 2010). In our more detailed model, conduit taper emerges as one of several influences on water use scaling,

underscoring the likelihood that selection on any single trait (like taper) can be relaxed by compensating changes in other variables (e.g. packing function, leaf hydraulics and sapwood area). Nevertheless, the boundaries of the Q_{ref} by q scaling space were finite and relate in context-specific ways to the same space-filling and safety vs. efficiency constraints emphasized by Savage *et al.*

The simulated scaling space excluded three-fourth intraspecific metabolic scaling. The greatest metabolic exponent was $c{\cdot}q = 0{\cdot}71$ and random sampling yielded an intraspecific mean $c{\cdot}q \approx 0{\cdot}63$. This mean is similar to the range predicted from observed water use scaling within the few tree species where it has been assessed (Mencuccini 2003; Meinzer *et al.* 2005). If metabolic scaling does indeed center on $c{\cdot}q = 0{\cdot}75$ as has been proposed (Enquist, Brown & West 1998; Enquist, West & Brown 2000; Niklas & Enquist 2001), the reason remains ambiguous based on our results.

Given the focus on three-fourth power scaling, we looked for situations where it could be consistent with the model and found two of them. Intraspecifically, if hydraulic conductance increases faster in roots than in shoots with size, q can reach or exceed 2 ($q \geq 2$) and $c{\cdot}q \geq 0{\cdot}75$. This pattern has been proposed as a mechanism to compensate for a potential hydraulic limitation on tree height (Magnani, Mencuccini & Grace 2000). However, data are limited and equivocal, with some species showing an increase in K/K_S with size (Martinez-Vilalta *et al.* 2007) and others not (von Allmen *et al.* 2012). A related explanation that applies to interspecific scaling is that species with greater inherent transport capacity (larger k_2 and/or q) would have less of a hydraulic limitation to height and grow taller than species with lower transport capacity. A bias for greater stature with steeper intraspecific scaling can theoretically give metabolic $c{\cdot}q$ exponents of 0·75 or higher (Fig. 5). While both scenarios are compatible with three-fourth power scaling, neither predicts that particular exponent from *a priori* optimization in the WBE sense.

Our species-level model is purposefully more complex and realistic than the Savage *et al.* analytical version. By allowing many functional traits to simultaneously vary, the numerical model reveals how a species' metabolic scaling results from interaction between complex trait interactions and covariance. A finite scaling space appears more realistic than convergence on one particular rule. This conclusion is based on a limited number of hydraulic traits, but is likely to be reinforced when additional complexities are considered. For example, the range of branching structure is more diverse than the generic WBE default (Price, Enquist & Savage 2007; L.P. Bentley, B.J. Enquist, V.M. Savage, P.B. Reich, D.D. Smith & J.S. Sperry, in review), carbon allocation may not always preserve isometry between metabolic sinks and vascular supply (Reich *et al.* 2006; Enquist *et al.* 2007b), and vascular supply itself would be modulated by dynamics of cavitation and refilling. Incorporating such complexity can translate an even broader diversity of plant functional traits into whole-plant performance. Such a framework could have general utility in ecology from constraining ecosystem fluxes and stocks to exploring the optimization of trait interactions.

Acknowledgements

The authors were supported by National Science Foundation Advancing Theory in Biology Award 0742800. J.S.S., D.D.S. and E.I.v.A. were partially funded by National Science Foundation Grant IBN-0743148. L.P.B. was also supported by NSF Postdoctoral Fellowship in Bioinformatics DBI-0905868.

References

Becker, P., Tyree, M.T. & Tsuda, M. (1999) Hydraulic conductances of angiosperm versus conifers: similar transport sufficiency at the whole-plant level. *Tree Physiology*, **19**, 445–452.

Enquist, B.J., Brown, J.H. & West, G.B. (1998) Allometric scaling of plant energetics and population density. *Nature*, **395**, 163–166.

Enquist, B.J., West, G.B. & Brown, J.H. (2000) Quarter-power allometric scaling in vascular plants: Functional basis and ecological consequences. *Scaling in Biology* (eds J.H. Brown & G.B. West), pp. 167–198. Oxford University Press, Oxford.

Enquist, B.J., Allen, A.P., Brown, J.H., Gillooly, J.F., Kerkhoff, A.J., Niklas, K.J., Price, C.A. & West, G.B. (2007a) Comment – Biological scaling: does the exception prove the rule? *Nature*, **445**, E9–E10.

Enquist, B.J., Kerkhoff, A.J., Stark, S.C., Swenson, N.G., McCarthy, M.C. & Price, C.A. (2007b) A general integrative model for scaling plant growth, carbon flux, and functional trait spectra. *Nature*, **449**, 218–222.

Hacke, U. & Sauter, J.J. (1996) Xylem dysfunction during winter and recovery of hydraulic conductivity in diffuse-porous and ring-porous trees. *Oecologia*, **105**, 435–439.

Hacke, U.G., Sperry, J.S., Pockman, W.P., Davis, S.D. & McCulloh, K.A. (2001) Trends in wood density and structure are linked to prevention of xylem implosion by negative pressure. *Oecologia*, **126**, 457–461.

Hacke, U.G., Sperry, J.S., Wheeler, J.K. & Castro, L. (2006) Scaling of angiosperm xylem structure with safety and efficiency. *Tree Physiology*, **26**, 689–701.

Hammond, S.T. & Niklas, K.J. (2012) Computer simulations support a core prediction of a contentious plant model. *American Journal of Botany*, **99**, 508–516.

van den Honert, T.H. (1948) Water transport in plants as a catenary process. *Discussions of the Faraday Society*, **3**, 146–153.

Horn, H.S. (2000) Twigs, trees and the dynamics of carbon in the landscape. *Scaling in Biology* (eds J.H. Brown & G.B. West), pp. 199–220. Oxford University Press, Oxford.

Hubbard, R.M., Stiller, V., Ryan, M.G. & Sperry, J.S. (2001) Stomatal conductance and photosynthesis vary linearly with plant hydraulic conductance in ponderosa pine. *Plant Cell and Environment*, **24**, 113–121.

Macinnes-Ng, C., Zeppel, M., Williams, M. & Eamus, D. (2011) Applying a SPA model to examine the impact of climate change on GPP of open woodlands and the potential for woody thickening. *Ecohydrology*, **4**, 379–393.

Magnani, F., Mencuccini, M. & Grace, J. (2000) Age related decline in stand productivity: the role of structural acclimation under hydraulic constraints. *Plant Cell and Environment*, **23**, 251–263.

Marks, C.O. & Lechowicz, M.J. (2006) Alternative designs and the evolution of functional diversity. *American Naturalist*, **167**, 55–66.

Martinez-Vilalta, J., Korakaki, E., Vanderklein, D. & Mencuccini, M. (2007) Below-ground hydraulic conductance is a function of environmental conditions and tree size in Scots pine. *Functional Ecology*, **21**, 1072–1083.

McCulloh, K.A., Sperry, J.S., Lachenbruch, B., Meinzer, F.C., Reich, P. B. & Voelker, S. (2010) Moving water well: comparing hydraulic efficiency in twigs and trunks of coniferous, ring-porous, and diffuse-porous saplings from temperate and tropical forests. *New Phytologist*, **186**, 439–450.

McMahon, T.A. (1973) Size and shape in biology. *Science*, **179**, 1201–1204.

Meinzer, F.C., Bond, B.J., Warren, J.M. & Woodruff, D.R. (2005) Does water transport scale universally with tree size? *Functional Ecology*, **19**, 558–565.

Mencuccini, M. (2002) Hydraulic constraints in the functional scaling of trees. *Tree Physiology*, **22**, 553–565.
Mencuccini, M. (2003) The ecological significance of long-distance water transport: short-term regulation, long-term acclimation and the hydraulic costs of stature across plant life forms. *Plant Cell and Environment*, **26**, 163–182.
Mencuccini, M., Hölttä, T., Petit, G. & Magnani, F. (2007) Sanio's laws revisited. Size-dependent changes in the xylem architecture of trees. *Ecology Letters*, **10**, 1084–1093.
Niklas, K.J. (1994) The allometry of safety-factors for plant height. *American Journal of Botany*, **81**, 345–351.
Niklas, K.J. & Enquist, B.J. (2001) Invariant scaling relationships for interspecific plant biomass production rates and body size. *Proceedings of the National Academy of Sciences of the United States of America*, **98**, 2922–2927.
Niklas, K.J. & Spatz, H.C. (2004) Growth and hydraulic (not mechanical) constraints govern the scaling of tree height and mass. *Proceedings of the National Academy of Sciences of the United States of America*, **101**, 15661–15663.
Pittermann, J., Sperry, J.S., Hacke, U.G., Wheeler, J.K. & Sikkema, E.H. (2005) Torus-margo pits help conifers compete with angiosperms. *Science*, **310**, 1924.
Pittermann, J., Sperry, J.S., Wheeler, J.K., Hacke, U.G. & Sikkema, E. H. (2006) Mechanical reinforcement of tracheids compromises the hydraulic efficiency of conifer xylem. *Plant Cell and Environment*, **29**, 1618–1628.
Price, C., Enquist, B.J. & Savage, V.M. (2007) A general model for allometric covariation in botanical form and function. *Proceedings of the National Academy of Sciences of the United States of America*, **104**, 13204–13209.
Reich, P.B., Tjoelker, M.G., Machado, J.L. & Oleksyn, J. (2006) Universal scaling of respiratory metabolism, size and nitrogen in plants. *Nature*, **439**, 457–461.
Richter, J.P. (1970) *The notebooks of Leonardo da Vinci, vol I*. Dover, New York.
Richter, H. (1973) Frictional potential losses and total water potential in plants: a re-evaluation. *Journal of Experimental Botany*, **274**, 983–994.
Ryan, M.G., Philips, N. & Bond, B.J. (2006) The hydraulic limitation hypothesis revisited. *Plant Cell and Environment*, **29**, 367–381.
Savage, V.M., Bentley, L.P., Enquist, B.J., Sperry, J.S., Smith, D.D., Reich, P.B. & von Allmen, E.I. (2010) Hydraulic trade-offs and space filling enable better predictions of vascular structure and function in plants. *Proceedings of the National Academy of Sciences of the United States of America*, **107**, 22722–22727.
Sperry, J.S., Meinzer, F.C. & McCulloh, K.A. (2008) Safety and efficiency conflicts in hydraulic architecture: scaling from tissues to trees. *Plant Cell and Environment*, **31**, 632–645.
Sperry, J.S., Nichols, K.L., Sullivan, J.E.M. & Eastlack, S.E. (1994) Xylem embolism in ring-porous, diffuse-porous, and coniferous trees of northern Utah and interior Alaska. *Ecology*, **75**, 1736–1752.
Sperry, J.S., Hacke, U.G., Comstock, J.P. & Oren, R. (2002) Water deficits and hydraulic limits to leaf water supply. *Plant Cell and Environment*, **25**, 251–264.
Tyree, M.T. (1988) A dynamic model for water flow in a single tree: evidence that models must account for hydraulic architecture. *Tree Physiology*, **4**, 195–217.
von Allmen, E.I., Sperry, J.S., Smith, D.D., Savage, V.M., Enquist, B.J., Reich, P.B. & Bentley, L.P. (2012) A species-level model for metabolic scaling of trees. II. Testing in a ring- and diffuse-porous species. *Functional Ecology*, doi: 10.1111/j.1365-2435.2012.02021.x.
West, G.B., Brown, J.H. & Enquist, B.J. (1997) A general model for the origin of allometric scaling laws in biology. *Science*, **276**, 122–126.
West, G.B., Brown, J.H. & Enquist, B.J. (1999) A general model for the structure and allometry of plant vascular systems. *Nature*, **400**, 664–667.
Wullschleger, S.D., Meinzer, F.C. & Vertessy, R.A. (1998) A review of whole-plant water use studies in trees. *Tree Physiology*, **18**, 499–512.
Zimmermann, M.H. (1978) Hydraulic architecture of some diffuse porous trees. *Canadian Journal of, Botany*, **56**, 2286–2295.
Zimmermann, M.H. (1983) *Xylem Structure and the Ascent of Sap*. Springer, Berlin.

Received 4 October 2011; accepted 17 May 2012
Handling Editor: Niels Anten

Supporting Information

Additional Supporting Information may be found in the online version of this article:

Appendix S1. I. Size-dependent water use allometry; II. functional tree types in scaling space; III. Intra- vs. inter-specific scaling.

As a service to our authors and readers, this journal provides supporting information supplied by the authors. Such materials may be re-organized for online delivery, but are not copy-edited or typeset. Technical support issues arising from supporting information (other than missing files) should be addressed to the authors.